PERGAMON

Vision Research 40 (2000) 459–472

Vision Research

www.elsevier.com/locate/visres

Perception of head orientation

Hugh R. Wilson [a,*], Frances Wilkinson [b], Li-Ming Lin [a], Maja Castillo [a]

[a] *Visual Sciences Center, University of Chicago, 939 East 57th Street, Chicago, IL 60637, USA*
[b] *Department of Psychology, McGill University, Montreal, Que., Canada*

Received 14 April 1999; received in revised form 7 September 1999

Abstract

There are two visual components to gaze: head orientation and orientation of the eyes relative to the head. This study explores the accuracy with which subjects can discriminate head orientation when the eyes are centered in the head. Discrimination thresholds averaged 1.9° of head rotation for base head orientations of 0° and 15°, but discrimination was markedly poorer around a 30° head orientation. Results were independent of spatial frequency and size over a 4-fold range. Neither negative contrast nor head inversion affected discrimination. Experiments dissociating the internal features from head outline revealed the presence of two main cues to discrimination: deviation of the head profile from bilateral symmetry, and deviation of nose orientation from vertical. Simulations show that model V4 units revealed in previous experiments with Glass patterns can extract the relevant head orientation information. The data are consistent with neurological data indicating a selective loss of face recognition in prosopagnosia with spared gaze discrimination.

Keywords: Face perception; Gaze discrimination; Pattern discrimination; Form vision; V4 model

1. Introduction

Perception of the direction in which another person's gaze is directed provides important visual cues to their focus of attention and to their social interactions. Indeed, gaze direction provides an important cue for inferring the intentions of other people, an ability sometimes referred to as 'mind reading' (Baron-Cohen, 1995). Gaze direction perception may be broken down into two components: perception of the direction in which the head is oriented, and perception of eye position relative to the head. Vectorial combination of these two factors using established neural networks for vector summation (Wilson, Ferrera & Yo, 1992; Wilson, 1999a) can then yield gaze direction information.

Of the two components of gaze direction, eye position within the head has received the most attention. Anstis, Mayhew and Morley (1969) provided evidence that the extent of visible sclera on either side of the iris is a major signal for determining gaze direction when the head is rotated away from the observer. Recent studies also have concluded that the relative amount of sclera visible to the left and right of the iris provides the major cue to eye direction when the face is pointed towards the observer (Ando & Osaka, 1998; Cedrone, Symons & Lee, 1998). In support of this, Kobayashi and Kohshima (1997) discovered that humans have more exposed sclera than other primates and are the only primates with a high contrast 'white' sclera. They conclude that: 'The uniqueness of human eye morphology among primates illustrates the difference between humans and other primates in the ability to communicate using gaze signals'.

The earliest psychophysical studies of gaze perception generally covaried head and eye direction to maintain fixation on the subject (Gibson & Pick, 1963; Cline, 1967; Anstis et al., 1969). These studies, in which eyes and head were counter-rotated to varying degrees, consistently showed an interaction between eye and head position in the perception of gaze direction. First, discrimination of gaze direction was most accurate when the head was pointed directly toward the subject, with JNDs of gaze direction of 0.75° (Cline, 1967) to 2.8° (Gibson & Pick, 1963) being obtained. Rotation of

* Corresponding author. Fax: +1-773-7024442.
E-mail address: hrw6@midway.uchicago.edu (H.R. Wilson)

0042-6989/00/$ - see front matter
PII: S0042-6989(99)00195-9

the head by 30° to the side consistently produced larger errors in discriminating gaze direction in all three studies. In addition, constant errors were observed such that the counter-rotated eye direction was overestimated in the direction opposite to the head orientation (Gibson & Pick, 1963; Anstis et al., 1969).

These classic studies have provided evidence for an interaction between head and eye gaze directions when the head is rotated significantly to the side. Furthermore, there is evidence that the perceived direction of eye gaze within the head is derived from the relative widths of sclera visible on either side of the iris. Only one study has reported data on the accuracy with which head orientation can be discriminated under conditions where the eyes are always pointed straight within the head (Troje & Siebeck, 1998). The experiments reported here complement and extend that work by quantifying the accuracy of head orientation discrimination under a range of conditions and exploring the visual cues to head orientation. The results show that discrimination is most accurate for a $\pm 15°$ range of forward gaze directions but deteriorates for a 30° head orientation. Thresholds are insensitive to both spatial frequency and head size within a 4-fold range. Furthermore, neither head inversion nor contrast negation had a significant effect on the results despite the fact that both these manipulations degrade face recognition (Bruce & Young, 1998). This suggests that the perceptual machinery subserving head orientation perception may utilize simpler and more universal aspects of face shape than are required for individual face recognition. This conclusion is supported by neurological evidence indicating a double dissociation between damage to face recognition and damage to gaze discrimination abilities (Campbell, Heywood, Cowey, Regard & Landis, 1990; Young, Aggleton, Hellawell, Johnson, Broks & Hainley, 1995). A final series of experiments provides evidence that subjects can utilize either of two cues to discriminate head orientation: deviation of head shape from bilateral symmetry, and deviation of nose orientation from vertical. Processing of heads by recently proposed global concentric (Wilson, Wilkinson & Asaad, 1997) and radial (Wilson & Wilkinson, 1998) units thought to exist in V4 (Gallant, Braun & VanEssen, 1993; Gallant, Connor, Rakshit, Lewis & VanEssen, 1996) provides a basis for extraction of these head orientation cues.

2. General methods

All stimuli were generated on an Apple Macintosh IIfx computer with gray scale monitor. Screen resolution was 640 (w) by 480 (h) pixels, which subtended 9.8° by 7.3° at the viewing distance of 1.25 m. The frame rate was 67 Hz, and the mean luminance was 46 cd/m^2. Intensity linearization was accomplished by selecting a subset of 151 luminance values (out of 256 total) that fell on a straight line with correlation greater than 0.994.

For all of the faces used in these experiments the eyes were directed straight ahead within the head, and only the orientation of the entire head was varied, so this will be termed head orientation. Thresholds for discriminating head orientation were measured using the method of constant stimuli in a two temporal interval forced choice paradigm. Viewing was binocular with the subject's head comfortably positioned in a chin rest. Each trial was initiated by a button press following which a base head orientation and one of four randomly chosen orientation increments were presented in random order. Each pattern was presented for 167 ms to prevent scrutiny involving eye movements. In addition, each stimulus was jittered in position from trial to trial by up to $\pm 0.3°$ (chosen from a uniform distribution) so that subjects could not anticipate exactly where any particular facial feature would appear. During the 500 ms interval between pattern presentations the screen returned to the mean luminance. The subject indicated the interval she thought contained the head orientation that was farthest from straight ahead by pressing an appropriate button. Each orientation increment stimulus was presented 32 times in random order, so each experiment contained 128 trials. Upon completion of the experiment the percentage of correct responses was computed as a function of orientation increment. The data were fit by a Quick (1974) or Weibull (1951) function using a maximum likelihood procedure, and the threshold was taken to be the 75% correct point estimated from this fit. All reported thresholds are means of three experimental replications.

A Kodak DC50 digital camera was used to photograph the heads of volunteers at a series of angles. Mean head width in the main experiments was 2.5° of visual angle, which corresponds to an average head viewed at approximately 3.5 m. The base head orientations used were 0° (direct front gaze), 15° and 30°. Increments about these base orientations were generated by having the model maintain a constant forward gaze while the camera was shifted successively to one side to produce a series of increasing deviations from each base orientation. Increments of 1.5°, 3.0°, 4.5° and 6.0° were used with the 0° and 15° base angles, while increments of 2°, 4°, 6° and 8° were used with the 30° base angle. Similar head orientation stimuli were made using three different faces, two female and one male, and subjects were tested once with each face (total of three replications) on each experimental condition.

Once the digital photographs had been made, they were transferred to a Power Macintosh for image processing using MatLab™ software. First, each image was bandpass filtered by convolution with a circular

difference of Gaussians filter (F) described in spatial coordinates (x, y) by the equation:

$$F(R) = 1.8\exp\left(\frac{-R^2}{\sigma^2}\right) - 0.8\exp\left(\frac{-R^2}{(1.5\sigma)^2}\right)$$

$$\text{where} \qquad R = \sqrt{x^2 + y^2} \tag{1}$$

This non-oriented filter has a spatial frequency bandwidth of 1.7 octaves at half amplitude and integrates to zero over the (x, y) plane. The space constant s was chosen to produce peak spatial frequencies of 4.0, 8.0, and 16.0 cpd at the 1.25 m viewing distance. Following bandpass filtering, the software vignetted the image to extract only the head, while replacing neck, shoulders, and background with the mean luminance of the screen. Finally, each stimulus was duplicated and flipped horizontally to produce a mirror image. Each experiment randomly interspersed normal and mirror image stimuli, so subjects had to make absolute judgments of increments from each base orientation independent of whether the head was oriented left or right of straight ahead. Examples of the resulting stimuli for the three base head orientations filtered at 8.0 cpd are depicted in Fig. 1.

The subjects in these experiments included the authors plus three experienced psychophysical observers who were otherwise naive concerning the goals of this research. All had normal or corrected to normal vision.

3. Experiment 1: effects of size and spatial frequency

As naturally occurring biological stimuli, human faces are seen and analyzed over a wide range of distances. At 1.0 m a typical face subtends about 8.0°, while at 25 m the same face would subtend about 0.32°. At the longer viewing distance, only five cycles of 16.0 cpd information would be present across the face, which approaches the limit for face processing given rapidly declining acuity at higher spatial frequencies (Tieger & Ganz, 1979). Given these ethological considerations, it therefore becomes important to determine how size and spatial frequency affect perception of head orientation.

3.1. Stimuli

In separate experiments three different base head orientations were used: 0°, 15° and 30°. These were combined with spatial frequency filtering (Eq. (1)) peaking at 4.0, 8.0, or 16.0 cpd, thus generating nine separate combinations of spatial frequency and head orientation, each of which was used in a separate experiment. Head width for these experiments averaged 2.5°. To determine effects of head width, experiments with the lowest peak frequency stimulus and 0° head orientation were replicated at twice and four times the viewing distance. This generated 1.25° wide heads filtered at 8.0 cpd and 0.625° wide heads filtered at 16.0 cpd.

3.2. Results

The data in Fig. 2 show discrimination thresholds for two subjects (solid versus open symbols) at base head orientations of 0°, 15° and 30°. Data for 4.0 cpd filtered stimuli are plotted as circles, 8.0 cpd data as squares, and 16.0 cpd data as diamonds. Two points are evident from the data in Fig. 2. First, head orientation discrimination thresholds are nearly constant from 0° to 15° base angles, but all thresholds rise substantially for the 30° base angle. Mean values of orientation discrimination threshold averaged across all conditions and subjects are 1.9°, 2.1° and 4.9°, respectively for base angles of 0°, 15° and 30°. Two further subjects were tested at 8.0 cpd and produced similar results. The second major result evident in the graph is the lack of any systematic dependence on spatial frequency over the 4.0 to 16.0 cpd range. An earlier study of face identification also showed no differential effect of mask spatial frequency over a substantial range (Moscovich & Radzins, 1987).

Fig. 1. Faces bandpass filtered at 8.0 cpd. The three base conditions of 0°, 15° and 30° head orientation are shown.

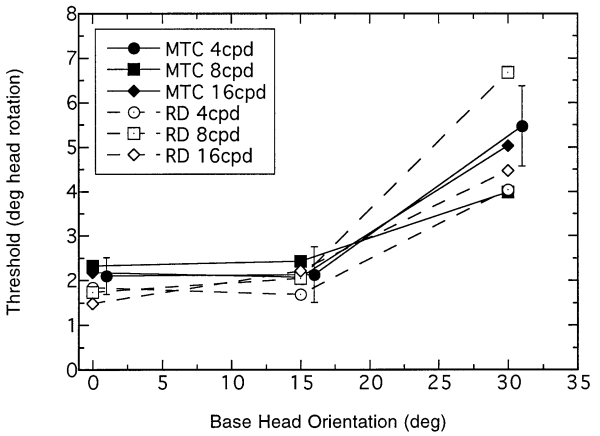

Fig. 2. Discrimination thresholds (degrees of head rotation) for two subjects (solid versus open symbols) as a function of base head orientation. Results for 4.0 cpd (circles), 8.0 cpd (squares), and 16.0 cpd (diamonds) are shown. Standard error bars plotted for one condition are typical of these data. For both subjects and all spatial frequencies discrimination was constant for the 0° and 15° base conditions but became significantly worse for the 30° base condition. There was no significant effect of peak spatial frequency.

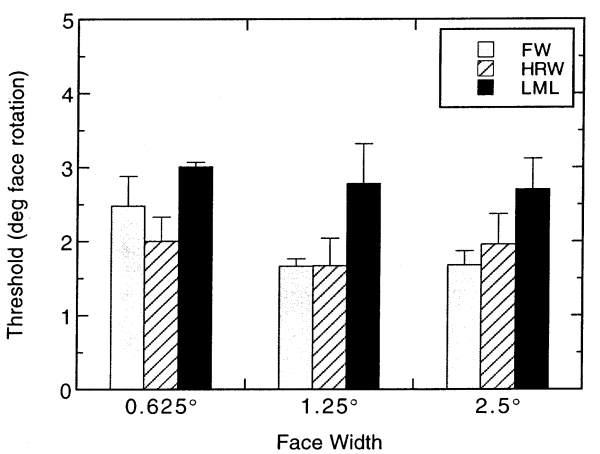

Fig. 3. Effects of head width on head orientation discrimination. Error bars plot the standard error of the mean. The 1.25° and 2.5° faces were bandpass filtered at 8.0 cpd, while the 0.625° faces had a peak spatial frequency of 16.0 cpd. There was no significant effect of head width over this range.

To assess any effects of head size, experiments at 0° head orientation were repeated for mean head sizes of 2.5°, 1.25° and 0.625°. Bandpass filtering peaked at 8.0 cpd for the 2.5° and 1.25° sizes, and at 16.0 cpd for the 0.625° head size. Data for three subjects are plotted in Fig. 3. There was no significant effect of face size ($F = 1.33$, $P > 0.30$), and there was no significant face size by subject interaction ($F = 0.34$, $P > 0.8$). The data thus establish that there is a 4-fold range of head sizes over which performance remains essentially constant. Accordingly, all subsequent experiments were conducted using 2.5° wide stimuli bandpass filtered at 8.0 cpd.

4. Experiment 2: effects of inversion and negative contrast

It is well documented that both up-down inversion (Yin, 1969; Tanaka & Farah, 1993) and negative contrast (Galper & Hochberg, 1971; Phillips, 1972) greatly interfere with face recognition. This experiment determined whether the same was true for discrimination of head orientation.

4.1. Stimuli

Three different types of stimuli were used: inverted faces, negative contrast faces, and faces that were both inverted and contrast negated. All stimuli were filtered at 8.0 cpd, had a mean width of 2.5° and a 0° base head orientation. An example of an inverted and negative contrast stimulus is depicted in Fig. 4.

4.2. Results

The effects of head inversion and negative contrast are plotted in Fig. 4. Subjects HRW and LML were tested in all three conditions, while FW and BK were only tested in the inverted plus negative contrast condition. Relative to the normal condition (i.e. normal contrast and orientation), the data show little or no effect of either inversion, negative contrast, or a combination of the two. Comparison of all four subjects between the normal condition and the combination of inversion and negative contrast showed that there was only an 18% increase in head orientation threshold between the two conditions averaged over subjects.

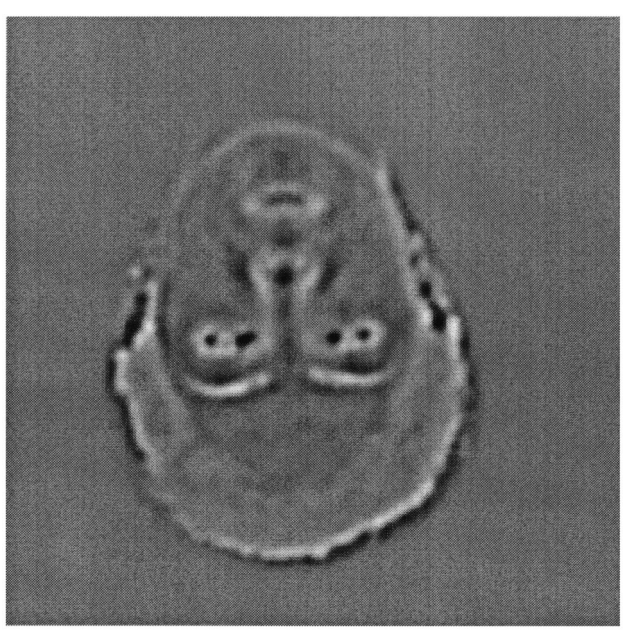

Fig. 4. Example of a 0° base head orientation that has been inverted and converted to negative contrast.

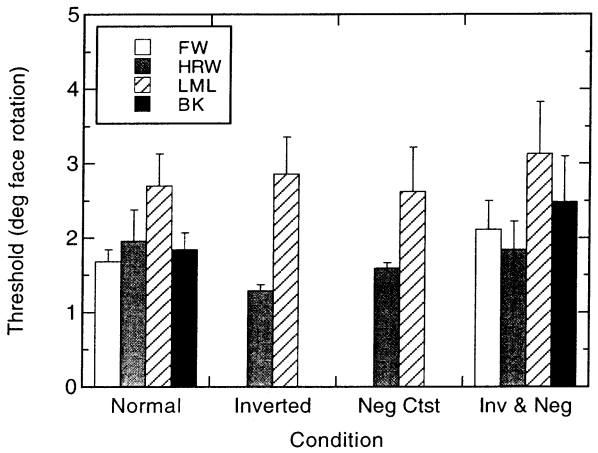

Fig. 5. Comparison of head orientation discrimination for normal, inverted, negative contrast, and the combination of inversion plus negative contrast conditions. All data were obtained in the 0° base orientation condition. Error bars plot standard errors of the mean. Neither head inversion, contrast negation, nor the combination of both produced a statistically significant effect.

Standard t-tests on each subject individually showed that there was no significant threshold elevation for any subject ($P > 0.15$ in every case). Data from the two subjects who were also measured on the inverted and negative contrast conditions separately show no effect of either condition in isolation (Fig. 5).

Our results show that neural mechanisms subserving head orientation discrimination are insensitive to either contrast polarity or head inversion. These results contrast sharply with the effects of these manipulations on face recognition, where negative contrast increases the error rate by a factor of 2–3 (Galper & Hochberg, 1971; Phillips, 1972), and inversion produces almost five times the error rate (Yin, 1969). Implications of these differences between head orientation perception and face recognition will be considered in Section 9.

5. Experiment 3: cues to head orientation discrimination

What cues do subjects use to discriminate head orientation? Our first conjecture was that it was probably a change in the configuration of internal features relative to the outline of the head. To test this, experiments were conducted with two separated face components: the internal features, and the head contour, similar to the approach to face matching employed by Young, Hay, McWeeny and Ellis (1985).

5.1. Stimuli

All stimuli were derived from 8.0 cpd filtered faces of 2.5° width and 0° base head orientation. Image processing using an author-designed MatLab™ program isolated internal facial features from the head contour along a smooth ovoid contour enclosing eyes, eye brows, nose, and mouth but excluding both hair and the head outline. The software then smoothly blended the edges of the feature region to the mean luminance of the screen using a Gaussian blur function (space constant of five pixels or 0.076°), which minimized visibility of the boundary of the feature region. Once the features had been isolated in this manner, the head contour was constructed by subtracting the features from the original face. As a result of this procedure, the head and the features added together exactly reproduce the original face. An example of a face along with its isolated features and head contour is illustrated in Fig. 6.

5.2. Results

Before conducting this experiment, our conjecture had been that head orientation discrimination depended on the inter-relations between head outline and internal features so that discrimination using either in

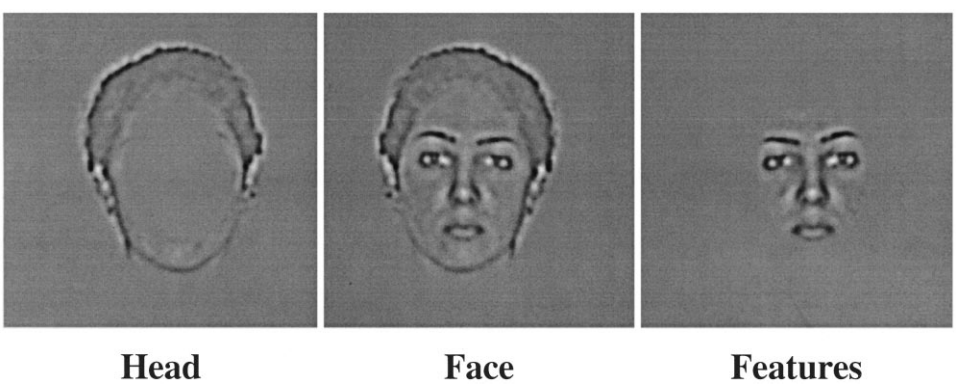

Fig. 6. Example of head contour and internal features stimuli extracted from the face in the center panel. The features plus the head exactly reproduce the original face. The cut between head and features was smoothed by a Gaussian tapered blur back to the mean luminance to minimize cut visibility.

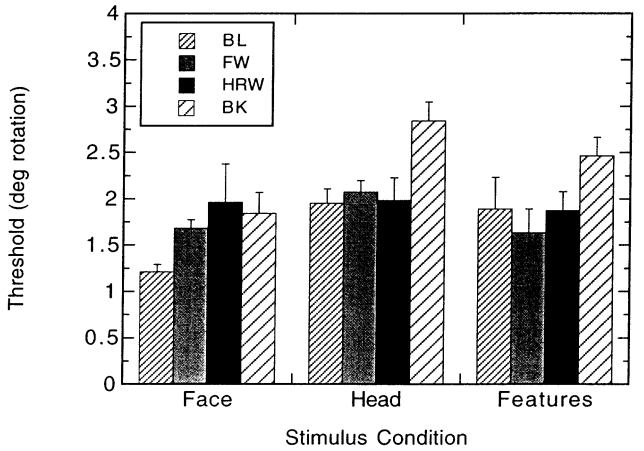

Fig. 7. Discrimination thresholds for the face, head, and features stimuli (see Fig. 6). Although two subjects (BL & BK) produced slightly higher thresholds for the head and features than for the entire face, a two-way ANOVA revealed no statistically significant effect of stimulus type on discrimination thresholds.

isolation would be quite difficult. The data plotted in Fig. 7 show that this is not correct, however. A two-way ANOVA showed that the difference between face, head, and features conditions was not significant ($F = 2.75$, $P > 0.09$). In addition, there was no significant interaction between subjects and the face parts.

The results of this experiment indicate that head orientation may be discriminated using either head shape or the internal features alone, and they demonstrate that these two sources provide cues of equivalent strength. The data are similar to those obtained by Young et al. (1985) showing that both head shape and internal features contribute to face matching. Averaged across subjects gaze thresholds were 1.67° (face), 2.21° (head), and 1.96° (features). For FW and HRW, thresholds for the entire face can be explained by the use of either the feature or the head contour information independently. For BK and BL the slightly lower thresholds for the entire face can be explained by probability summation between the cues present in the features and head shape. An exponent of 3.0 in the standard Quick (1974) formula provides a good fit to their thresholds.

6. Experiment 4: surrogate nose orientation discrimination

What cue is used for discrimination using internal features? Among the internal features there are two major changes that occur as the face is rotated slightly from straight ahead: a decrease in the inter-ocular distance, and a deviation of the nose orientation away from vertical. Decrease in the inter-ocular distance can be calculated easily (it is too small to be measured on the stimuli). The mean distance between the eyes in the 0° base condition was 0.77°. The change in the inter-ocular distance for a head rotation of 1.96° (the mean threshold for the features condition) is easily calculated from trigonometry to be 1.6 arc sec. Measured separation discrimination thresholds for elements separated by 0.77° fall in the range 50–60 arc sec (Burbeck, 1987; Levi, Klein & Yap, 1988). Therefore, the change in inter-ocular separation at the discrimination threshold for features is at least 30 times too small to be detected by the visual system. The same considerations lead to rejection of changes in mouth width as a possible cue for gaze discrimination at small deviations from 0°.

As discrimination of feature gaze direction cannot be derived from variations in inter-ocular distance, the remaining candidate is deviation of nose orientation from vertical. By measuring nose orientation in our stimuli it was found that the mean orientation deviated from vertical by an average of 1.68° at the threshold for orientation discrimination using features. This is somewhat larger than typical orientation discrimination thresholds of about 0.5° (e.g. Orban, Vandenbussche & Vogels, 1984; Burr & Wijesundra, 1991; Lin & Wilson, 1996). Accordingly, orientation discrimination was measured using stimuli with dimensions comparable to the noses in our study ('surrogate noses').

6.1. Stimuli

As a surrogate vertical nose filtered at 8.0 cpd, we used an elongated difference of Gaussians (DOG) described by the equation:

$$\mathrm{DOG}(x,y) = C\left[3\exp\left(\frac{-x^2}{\sigma^2}\right) - 2\exp\left(\frac{-x^2}{2.25\sigma^2}\right)\right]\exp\left(\frac{-y^2}{\lambda^2}\right) \quad (2)$$

Other orientations were obtained by rotation of coordinates. Measurements of the features stimuli showed that the nose contrast averaged across faces was $C = 0.373 \pm 0.011$, so this value was used for C in Eq. (2). The space constant $\sigma = 0.032°$ for a peak spatial frequency of 8.0 cpd, and the length constant was set to $\lambda = 0.27°$ so that the 1/e to 1/e length of the DOG was equal to the mean nose length of 0.54° measured from the stimuli. Orientation thresholds were measured using this surrogate nose with the same $\pm 0.3°$ position jitter and 167 ms presentations used for all other stimuli in this study.

6.2. Results

Thresholds for discrimination of deviations from vertical were similar across subjects and averaged $1.54 \pm 0.22°$. This value is not significantly different from the 1.68° deviation of the nose from vertical at threshold in

the feature condition. These experiments were replicated using the mean nose orientation of 14.4° derived from the 30° baseline condition. In agreement with the literature (Regan and Price, 1986), discrimination thresholds rose to an average of $3.65 \pm 0.41°$. This figure is close to the 3.84° change in nose orientation at threshold in the 30° baseline condition. These data provide strong evidence that nose orientation is the cue for gaze direction based on internal features.

7. Experiment 5: head contour symmetry discrimination

For the head contour stimuli the only obvious cue is distortion of the contour as the head is rotated away from the 0° base condition. This distortion may be thought of as an increasing deviation from (approximate) bilateral symmetry. To test this hypothesis, we generated surrogate head shapes using the radial frequency (RF) patterns introduced by Wilkinson, Wilson and Habak (1998).

7.1. Stimuli

Radial frequency patterns are defined in polar coordinates such that the radius R of a smooth closed contour varies about a mean R_0 as a cosine function of polar angle θ with frequency ω, phase ϕ_ω and amplitude A_ω:

$$R_\omega(\theta) = R_0 + A_\omega \cos(\omega\theta + \phi_\omega) \quad (3)$$

A bandpass Fourier spectrum for the contour defined by $R_\omega(\theta)$ is produced by causing the contour cross-section to vary as the fourth derivative of a Gaussian (see Wilkinson et al., 1998, for details and illustrations). As first observed by Lu (1965), the shape of human heads can be accurately described by a sum of several functions described by Eq. (3) with different frequencies ω. Furthermore, deviations from bilateral symmetry may be precisely quantified by variations of the phases ϕ_ω. We have found that a sum of five RF functions produces a good representation of head shape:

$$R_{\text{head}}(\theta) = R_0 + \sum_{\omega=1}^{5} A_\omega \cos(\omega\theta + \phi_\omega) \quad (4)$$

Measurement of the radius of our head stimuli from the bridge of the nose to each of 12 evenly spaced radial points around the circumference of the head followed by a five term Fourier analysis permitted us to determine the values of A_ω and ϕ_ω for $\omega = 1 \ldots 5$. To generate a mean head shape from our stimuli for the 0° baseline condition, A_ω values were averaged across heads, and mean ϕ_ω values were set to the nearest angles that would produce bilateral symmetry. The resulting surrogate head with an 8.0 cpd peak frequency is shown in the middle of Fig. 8.

Similar measurements on heads rotated from the 0° baseline condition confirmed that the only significant change was in the phases ϕ_ω and not in the amplitudes. Furthermore, only the phases for $\omega = 1$ and 3 changed significantly, with the others remaining constant. The phases of both these terms could be described by the equation:

$$\phi_{1,3} = \pi/2 \pm 0.073\Omega \quad (5)$$

where Ω is the angular rotation of the head away from the 0° base condition either to the right (+) or to the left (−). Examples of surrogate heads rotated by ± 4.0° based on Eq. (5) are illustrated in Fig. 8.

7.2. Results

Thresholds for the radial frequency patterns from Eq. (4), plotted as degrees of rotation based on W in Eq. (5), are plotted as dark gray bars in Fig. 9. For each subject the light gray bar replots the head contour data from Fig. 7. Lower thresholds were produced for the RF patterns than for the heads for all subjects, and this difference was statistically significant for all except HRW. Averaged across subjects, RF thresholds were

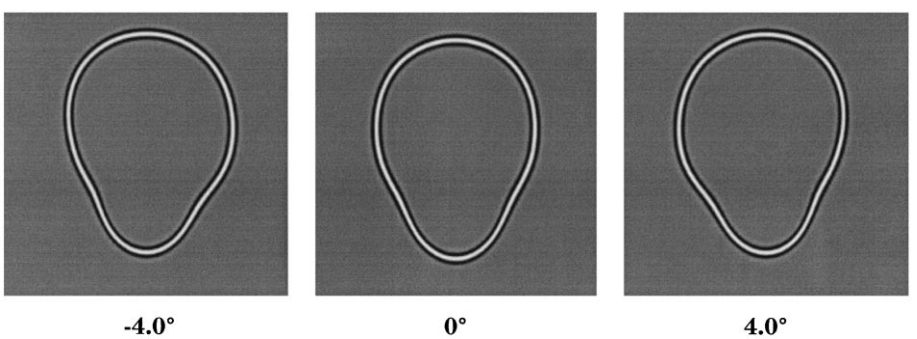

Fig. 8. Examples of surrogate head shapes produced by the summation of five RF patterns according to Eqs. (4) and (5). These RF patterns were based on measurements of the mean human head shape used in previous experiments. The center pattern shows the bilaterally symmetric 0° base condition, while the ± 4.0° RF patterns incorporate deviations from bilateral symmetry that would be produced by these angular deviations of gaze. See text for further details.

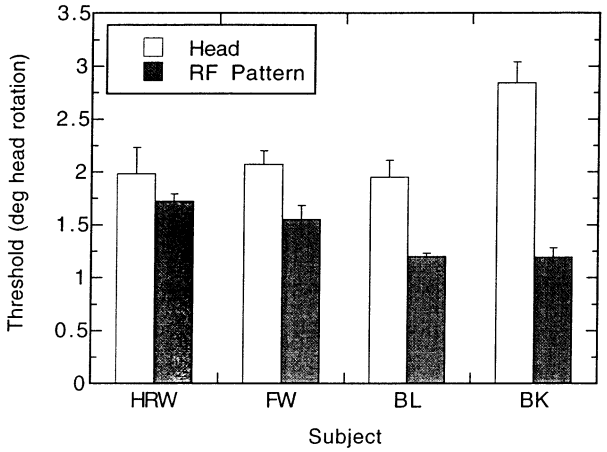

Fig. 9. Discrimination thresholds for head contours (see Fig. 6) and the RF patterns in Fig. 8. Thresholds for the RF patterns (dark gray) were significantly lower than thresholds for discriminating head orientation (light gray) for all subjects except HRW. This improvement with RF patterns is likely due to their perfect bilateral symmetry in the 0° base condition compared to imperfect bilateral symmetry of the actual head contours.

1.42°, and head thresholds were 2.21°. An important observation here is that the RF pattern experiments required subjects to discriminate patterns with exact bilateral symmetry from those deviating from symmetry. In the discrimination of head contours derived from our face stimuli, however, the 0° base condition was never exactly bilaterally symmetric, as human faces always deviate somewhat from perfect symmetry. Measurements of our stimuli confirmed small deviations from bilateral symmetry in the 0° base condition. Discrimination of deviations from such imperfect symmetry would certainly produce larger thresholds than deviations from perfect symmetry. Thus, the data here are consistent with symmetry discrimination as the basis for gaze discrimination with the head contours.

8. A neural model for head orientation discrimination

The data presented above support the contention that there are two cues to head orientation: deviation of head outline from bilateral symmetry, and deviation of nose orientation from vertical. But how are these cues extracted from the visual image of a head by cortical circuits? It might seem obvious that the orientation of the nose is determined by locating the nose and using the responses of orientation specific cells to measure its location, but this begs the question: how does the cortical form vision system localize the nose in the first place? While a definitive answer is not possible yet, a plausible explanation can be offered in terms of configuration sensitive units for which there is already extensive evidence. Gallant et al. (1993, 1996) documented the existence of two classes of neurons in primate area V4 that were optimized, respectively for detection of either concentric or radial gratings. Similar results, obtained using a totally different paradigm, were reported by Kobatake and Tanaka (1994).

Recent psychophysical studies provide evidence for the existence of configural units sensitive to concentric and radial structure in human vision, and quantitative neural models of these units have been developed (Wilson et al., 1997; Wilkinson et al., 1998; Wilson & Wilkinson, 1998). As the psychophysical results are consistent with the V4 physiology just summarized, these units will be termed V4 concentric and radial units. These units are constructed from oriented V1 filter responses followed by full-wave rectification and subsequent oriented filtering, a theme common to both texture and second order motion analysis (Wilson, 1999b). A final, concentrically organized summation of these responses completes the model for V4 configural units. When first and second stage filters have orthogonal orientations, the combination extracts local curvature (Dobbins, Zucker & Cynader, 1987; Koenderink & Richards, 1988; Dobbins, Zucker & Cynader, 1989; Wilson & Richards, 1992), so the final V4 summation stage pools concentric curvature information (Wilson et al., 1997). When the first and second stage filter orientations are parallel, radial structure is extracted by the model (Wilson & Wilkinson, 1998). To process the 8.0 cpd filtered faces, parameters for model V1 oriented filters peaking at 8.0 cpd were chosen based on previous masking studies (Wilson, 1991). These filters have a 1.3 octave spatial frequency bandwidth and a $\pm 15°$ orientation bandwidth. The mathematical description and parameters for the second stage oriented filters were taken from those employed by Wilson et al. (1997) but scaled towards higher spatial frequencies by a factor of 2.0. Thus, all parameters were appropriately scaled to produce an 8.0 cpd V4 concentric unit model. Finally, a contrast gain control was incorporated as part of the simulated V1 processing. This was accomplished by dividing each V1 filter response by $(1 + R_{\text{mean}})$, where R_{mean} is the mean of all V1 oriented responses averaged over a Gaussian window with space constant of 0.027°.

The concentric V4 model was applied to the stimuli from our study, and one example is depicted in Fig. 10. The location of the most strongly activated V4 concentric unit is indicated by the large black square in the lower center of the forehead. The most strongly activated unit can be determined by a regional winner-take-all competition among concentric units, and there is now psychophysical support for such competition (Wilson, Krupa & Wilkinson, 1999). The array of 12 smaller black squares surrounding the center one indicates locations of neighboring concentric units which comprise second nearest neighbors in an hexagonal lattice. Responses of these units to the head in Fig. 10 are plotted in polar coordinates by solid circles in Fig.

Fig. 10. Results of analyzing a face stimulus in the 0° base condition using the concentric V4 unit model of Wilson et al. (1997). Although the face is not centered, as was the case due to position jitter in the experiments, the maximum concentric unit response occurred at the center of the head (large black square). The 12 smaller squares are all at the same distance from the center square and show locations of neighboring concentric units envisioned as forming the second ring of an hexagonal lattice. Responses of the marked units are plotted in the next figure.

11A. These responses provide a sparse population code for overall head shape as well as the shapes of other ellipsoidal patterns (Wilkinson et al., 1998). This point is accentuated by the open circles in Fig. 11A, which show the results of applying the same neural model to a second face. This neural population code clearly differentiates the overall shapes of these heads.

Experiments 3 and 5 indicate that subjects can use deviations of head shape from bilateral symmetry to discriminate head orientation. The model V4 responses in Fig. 11A were both obtained from the 0° baseline condition (see Fig. 10), and it is evident that the model V4 population codes are almost bilaterally symmetric and specify the axis of facial elongation. This neural population code deviates from bilateral symmetry with gaze direction as illustrated in Fig. 11B. Here the model response depicted by open circles in Fig. 11A for the 0° condition is compared with model responses to the same face with gaze deviated by 6° (●). Neural responses to the 6° deviated face are clearly skewed away from bilateral symmetry.

In order to quantify asymmetries in the model response, an Asymmetry Index (AI) was calculated. First, the maximum of the 12 model responses surrounding the centered response was used to determine an approximate symmetry axis. For every one of the stimuli processed this turned out to be vertical. Designating the five model responses on the right as R_1 to R_5 and those on the left as L_1 to L_5 (all indexed relative to the response location defining the symmetry axis), the AI was defined as:

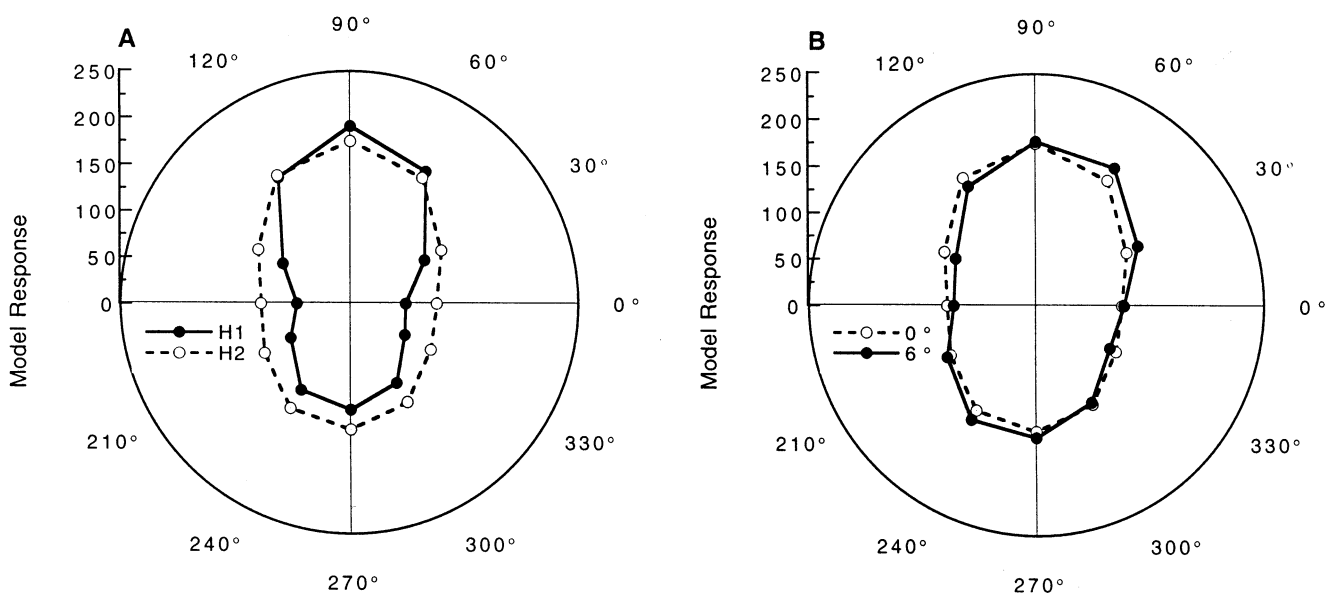

Fig. 11. Polar coordinate plots of model V4 concentric units to face stimuli used in the experiments. The solid circles in A show responses to the face in Fig. 10 at the 12 locations equally spaced around the locus of maximum activity. ○ show model responses to a second face from this study, also in the 0° base condition. These model responses produce a sparse population code reflecting differences in head shape. Note that the unit responses encode the vertical axis of face elongation and are almost bilaterally symmetric about this axis. Panel B replots the 0° base responses for one face from A (○) along with responses when the face gaze had shifted to 6° (●). The solid circles are skewed away from the more symmetric responses produced by the 0° condition.

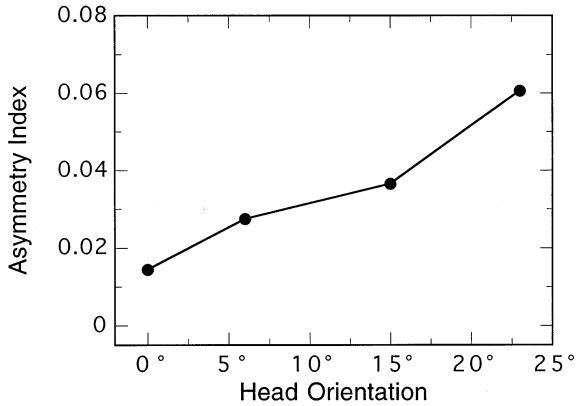

Fig. 12. Asymmetry index (AI) from Eq. (6) computed using the model V4 concentric unit network. Computed data points are averages across stimuli used in this study. The model AI increases approximately linearly over the range of head orientations shown and thus could provide a reliable basis for head orientation discrimination to about 20°. For reference, the perfectly symmetric 0° RF pattern in Fig. 8 produced an AI = 0.

$$\mathrm{AI} = \frac{\sum_{n=1}^{5} |L_n - R_n|}{\sum_{n=1}^{5} (L_n + R_n)} \tag{6}$$

AI = 0 when the neural responses indicate perfect bilateral symmetry, while in an extreme asymmetry case where $R_n = 0$ and $L_n > 0$ for all n, AI = 1. To confirm the adequacy of this formula, the perfectly symmetric RF surrogate head from experiment 5 was processed by the V4 model, and it produced an AI = 0. Accordingly, the 8.0 cpd filtered faces used in our main experiments were processed and the AIs calculated. Mean results are plotted in Fig. 12, which shows that AI rose monotonically and almost linearly as head orientation varied from 0° to 23°. It should be noted that AI in Eq. (6) can easily be computed by a neural network using responses of the V4 model: the numerator only requires subtractive inhibition, while the denominator represents a common form of gain control.

These results demonstrate that model V4 concentric units can locate the centroid and symmetry axis of a face and can encode deviations of the head outline from bilateral symmetry as the face is rotated away from a direct frontal view. While previous models of symmetry perception (e.g. Labonté, Shapira, Cohen & Faubert, 1996; Zabrodsky & Algom, 1996) might also succeed in extracting the relevant information from faces, the recent fMRI demonstration that fusiform face areas are also activated by concentric gratings lends further support to the putative role of V4 concentric units in face analysis (Wilkinson, James, Wilson, Gati, Menon & Goodale, 1999).

Regarding the second cue to gaze direction, namely deviation of nose orientation from vertical in the feature stimuli, the radial V4 model suggests a solution. Processing of feature stimuli by the radial V4 model shows that the maximal response is always located at the bridge of the nose, and this occurs independent of gaze direction from 0° to 30°. In detecting the bridge of the nose, model radial units pool the horizontal orientations present in the eye brows and lids together with the predominantly vertical information defining the nose itself, and this information is radially organized around the bridge of the nose. With this location as a cue, neural assessment of nose orientation becomes a simple task of sampling near vertical unit responses below the bridge of the nose. It is important to note here that concentric V4 units produce a maximal response in the center of the head, and this seldom coincides with the bridge of the nose, so the additional information provided by model V4 radial units is necessary to localize the nose in facial images.

9. Discussion

As early as 1824, Wollaston demonstrated that small changes of nose orientation in line drawings significantly altered the perception of head orientation (cited in Bruce & Young, 1998), and Troje and Siebeck (1998) have recently provided evidence for the use of a head asymmetry cue to gaze. The experiments reported above support the conclusion that head orientation discrimination is based upon both cues: deviation of head shape from bilateral symmetry, and deviation of nose orientation from vertical. These cues were found to be equally effective over a 4-fold range of size and spatial frequency, and they were insensitive to either contrast negation or face inversion. Finally, these cues can be extracted by models of global configural units optimized for either concentric or radial image structure (Wilson et al., 1997; Wilson & Wilkinson, 1998). Physiological (Gallant et al., 1993; 1996; Kobatake & Tanaka, 1994) and fMRI (Wilkinson et al., 1999) results support the existence of such units in V4, a higher area in the cortical form vision system.

The V4 concentric unit model applied to faces here was derived from data showing essentially perfect linear summation of concentric information in Glass (1969) patterns (Wilson et al., 1997). Kovács and Julesz (1993, 1994) independently demonstrated the salience of circular shapes using a radically different paradigm. Thus, there is convergent evidence for the operation of visual processes particularly sensitive to quasi-circular configurations.

Independence of head orientation discrimination over a range of sizes and spatial frequencies has obvious ethological significance, as it indicates that this discrimination is independent of viewing distance over a considerable range. For the range of face sizes used in our study this independence corresponds to viewing dis-

tances ranging from 3.5 m (2.5° wide faces) to 14.0 m (0.625° wide faces). As a head orientation threshold of 1.9° is slightly less than the width of a human face at 3.5 m, humans can discriminate gaze focused on adjacent faces up to this distance. Discrimination performance will certainly degrade when faces become too much smaller and for much higher or lower spatial frequencies, but social interactions are usually not carried on at great distances. In this context, it is worthy of note that perception of RF patterns (see Eq. (3)), to which the human visual system is exquisitely sensitive, has also been shown to exhibit almost perfect size constancy over a wide range of sizes and spatial frequencies (Wilkinson et al., 1998).

Bandpass filtered faces were used in this study for two reasons. First, bandpass filtering reduces relatively uniform areas of the face, the forehead and cheeks, to the mean luminance. Consequently, the contour between the head and features in Fig. 6 was rendered minimally visible. This would not have occurred had the original gray scale faces been subdivided into head and features without previous bandpass filtering.

More importantly, given the overwhelming evidence that primary visual cortex extracts orientation information in parallel on several different size or spatial frequency scales (DeValois & DeValois, 1988; Graham, 1989; Wilson, 1991), it becomes important to determine how this information is subsequently combined to extract meaningful information about the visual environment. Our results indicate that pooling of orientation information on a single spatial frequency scale is sufficient to determine head orientation. This is consistent with physiological evidence that neurons in V4 pool orientation information (Gallant et al., 1993, 1996; Kobatake & Tanaka, 1994; Schoups, Tootell, Vanduffel & Orban, 1995), yet V4 spatial frequency bandwidths remain the same as those in V1 (Desimone & Schein, 1987). Furthermore, meaningful configural pooling of orientation information would require relatively large receptive fields, and V4 receptive fields are four to seven times the diameter of those in V1 (Desimone & Schein, 1987).

Bandpass filtering raises an important question: would head orientation discrimination have been significantly better had the original, unfiltered gray scale facial images been used? An answer to this is provided by the results of Troje and Siebeck (1998). They studied the perceived head orientation of gray scale faces obtained by laser scanning. For a 0° base direction their mean gaze discrimination threshold, when converted from 84 to 75% correct, was 1.25°, but it rose to about 3.3° for the 30° base condition. This is the same pattern exhibited by our subjects in Fig. 2. Thresholds reported by Troje and Siebeck (1998) are slightly lower that those in Fig. 2, but two differences in stimulus presentation may explain this. They used a significantly longer presentation time (0.5 s for the first interval and unlimited for the second), and consequently they did not introduce the $\pm 0.3°$ position jitter present in our study. Finally, their lower thresholds are consistent with probability summation across spatial frequencies in our study. These comparisons indicate that no significant losses in gaze discrimination are produced by bandpass filtering, at least when using the 1.7 octave bandwidth filter in Eq. (1). Thus, head orientation can be effectively computed by the visual system with information restricted to a single spatial frequency scale. As the Troje and Siebeck (1998) faces were approximately 4.2° in width, their data in conjunction with ours extend the range of size constancy for gaze discrimination from about 2.0 to 14.0 m.

Hayes, Morrone and Burr (1986) have reported that identification of negative contrast faces is affected by bandpass filtering. They found that the performance deficit produced by negative contrast was present only for low spatial frequencies but not for high. However, this resulted from an identification decrease for high frequency filtered positive images down to the level of their negative contrast counterparts. The discussion above indicates that head orientation discrimination is comparable for both original gray scale and bandpass filtered images. Given the lack of any effect of contrast negation in experiment 2, therefore, it follows that filtered, negative contrast faces support gaze discrimination as well as normal gray scale faces. Accordingly, the absence of a contrast negation effect in experiment 2 seems to be due to the head orientation computation itself rather than to bandpass filtering of the face. Further differences between head orientation discrimination and face identification are considered below.

The degradation of head orientation discrimination in the 30° baseline condition is consistent with previous data showing increased errors in gaze perception when the head is rotated 30° to the side (Gibson & Pick, 1963; Cline, 1967; Anstis et al., 1969). As those studies covaried head rotation with counter-rotation of the eyes, the current results suggest that the larger errors in the 30° condition may be due to degraded discrimination of head orientation alone rather than to inaccuracies in discrimination of eye orientation as well. A plausible explanation of the discrimination deficits evident at 30° may be offered based on the two cues for discrimination in the 0° base condition: deviations from head bilateral symmetry and deviations of nose orientation from vertical. First, it is likely that the 30° face orientation is sufficiently asymmetric that symmetry calculations on head shape are no longer effective for gaze discrimination (we did not test this experimentally, because one eye, the tip of the nose, and the corner of the mouth fall too close to the head contour to permit effective isolation of the head contour, see Fig. 1). This suggests that nose orientation might be the principal cue in this case. Measurements of the stimuli indicated

that mean nose orientation deviated from vertical by 14.4° in the 30° face rotation condition. Measurements with the surrogate noses in experiment 4 confirmed that orientation discrimination around 14.4° rose to 3.65° ± 0.41°, which is similar to the computed nose orientation shift of 3.84° for the 30° baseline condition. These considerations may explain the degradation of gaze discrimination at 30°.

The use of bilateral head symmetry and deviations of the nose from vertical as cues to head orientation near 0° may be linked to another observation concerning face symmetry: bilaterally symmetric faces are perceived as more attractive than those deviating significantly from bilateral symmetry (Langlois & Roggman, 1990; Thornhill & Gangestad, 1993; Bruce & Young, 1998). Because only a vertical nose in front view can truly preserve bilateral symmetry of the entire face, both cues for discrimination of gaze direction are optimized in a symmetric face. As deviations of gaze direction provide a major cue to another's focus of attention, it is plausible that facilitation of gaze discrimination in symmetric faces is one ingredient underlying association of increased symmetry with enhanced attractiveness. Indeed, those with attractive faces are perceived as being more honest and generally socially appealing personalities (Bull & Rumsey, 1988; Bruce & Young, 1998). As difficulties in perceiving gaze direction can lead to difficulties in determining another's focus of attention (Baron-Cohen, 1995), it is not surprising that deviations from facial symmetry are regarded as both less attractive and more likely to be associated with a surreptitious personality.

Neither contrast negation nor face inversion significantly reduced the ability to discriminate head orientation. This is consistent with use of nose orientation and bilateral head symmetry cues, as neither of these tasks is sensitive to either inversion (which preserves symmetry axis orientation) or contrast reversal. However, these results differ dramatically from face recognition studies, where both contrast negation and face inversion reduce performance by several hundred percent (Yin, 1969; Galper & Hochberg, 1971; Phillips, 1972; Tanaka & Farah, 1993; Bruce & Young, 1998). A third difference between face recognition and our head orientation results is that face recognition is aided by views near 30° (Troje & Bülthoff, 1996; Bruce & Young, 1998), while gaze discrimination is degraded at the same angle. There is thus a consistent psychophysical dissociation between face recognition and gaze discrimination. Strikingly, evidence from both primates and humans with selective cortical lesions indicates a double dissociation between gaze perception and face recognition. Campbell et al. (1990) reported that monkeys with STS lesions were mainly deficient in perception of gaze direction. In addition, they found that one human prosopagnosic was unable to perceive gaze direction, while another was normal on a face gaze task. Young et al. (1995) reported that a bilateral amygdalotomy patient was normal at face recognition but deficient in perceiving gaze direction. This double dissociation in the neurological literature is consistent with the psychophysical data on face gaze as opposed to face recognition, and it suggests that there may be distinct cortical modules for gaze and recognition of faces. Certainly gaze direction entails a much simpler computation that can be performed with significantly less information.

Insensitivity of gaze discrimination to contrast negation suggests that full-wave rectification is involved in the neural computation. Wilson et al. (1997) reported direct evidence for full-wave rectification in the extraction of global concentric structure from Glass (1969) patterns. The V4 concentric model derived from that study therefore incorporates rectification and was used to produce the results in Figs. 10–12. Full-wave rectification in processing head shape and symmetry would be advantageous by rendering the computation independent of whether the head was viewed in front of a lighter or darker background. Obviously, however, contrast sign preserving operations must be involved in face recognition, or contrast negation would not cause such dramatic recognition deficits. The contrast gain control also makes the V4 model largely independent of local contrast throughout the pattern. Indeed, simulations showed that the asymmetry index for the perfectly symmetric RF head used in experiment 5 remained less than 0.002 even when RF contrast was smoothly varied by a factor of 1.8 across the face. This indicates that the V4 model would be able to compute head orientation independent of modest changes in lighting direction.

Troje and Siebeck (1998) observed shifts of up to 9° in apparent head orientation in the direction opposite to a powerful light source positioned to one side. This effect depended upon a change in the visible edge of the shadowed side of the head when viewed against a black background and largely disappeared when the background was light so as to reveal the true head outline. Accordingly, Troje and Siebeck (1998) attributed their effect to a global computation of head asymmetry relative to the profile line (i.e. the line through the forehead, bridge and tip of the nose, lips, etc.). Our results thus concur that computations of head asymmetry are one major cue to head orientation, but the data also support deviations of nose orientation from vertical as a second and independent cue. Our initial conjecture had been that asymmetry calculations were based on calculating location of the bridge of the nose relative to the head outline. For the 0° baseline condition, however, the results of experiment 3 do not support this, as effective discrimination may be obtained using the head contour alone. It may well be, however, that the computation suggested by Troje and Siebeck (1998) is employed for 30° and larger base conditions where

their measured gaze shift was most pronounced. In this regard, the head shape codes produced by model V4 concentric units in Fig. 11 would be distorted by dramatic side lighting against a black background, which might explain the shift of perceived gaze direction observed under these conditions.

The V4 concentric unit model proposed to explain discrimination of head asymmetry is supported by both physiological (Gallant et al., 1993, 1996; Kobatake & Tanaka, 1994) and psychophysical data (Wilson et al., 1997; Wilson & Wilkinson, 1998). Current fMRI evidence also indicates that concentric gratings produce significant stimulation of fusiform face areas in humans whereas sinusoidal gratings do not (Wilkinson et al., 1999). This supports the contention that these units are involved in aspects of face processing. As shown in Fig. 11A, the population codes produced by these units differ for differing head shapes. As head shape is an important element in face recognition (Young et al., 1985; Sinha & Poggio, 1996; Bruce & Young, 1998), this suggests that V4 concentric units may contribute to face recognition codes as well as to the computation of head orientation. If so, this would begin to explain how configural orientation pooling in V4 provides a computational substrate for higher level form vision.

Acknowledgements

Portions of this research were first reported at the Annual Meeting of the Association for Research in Vision and Ophthalmology, May 1998. This research was supported in part by NIH grant EY02158 to HRW and by NSERC grant OGP0007551 (Canada) to FW.

References

Anstis, S. M., Mayhew, J. W., & Morley, T. (1969). The perception of where a face or television 'portrait' is looking. *American Journal of Psychology*, *82*, 474–489.

Baron-Cohen, S. (1995). *Mindblindness*. Cambridge: MIT Press.

Bruce, V., & Young, A. (1998). *In the eye of the beholder: the science of face perception*. Oxford: Oxford University Press.

Bull, R., & Rumsey, N. (1988). *The social psychology of facial appearance*. New York: Springer.

Burbeck, C. A. (1987). Position and spatial frequency in large scale localization judgments. *Vision Research*, *27*, 417–427.

Burr, D. C., & Wijesundra, S. A. (1991). Orientation discrimination depends on spatial frequency. *Vision Research*, *31*, 1449–1452.

Campbell, R., Heywood, C. A., Cowey, A., Regard, M., & Landis, T. (1990). Sensitivity to eye gaze in prosopagnosic patients and monkeys with superior temporal sulcus ablation. *Neuropsychologia*, *28*, 1123–1142.

Cedrone, C. C., Symons, L. A., & Lee, K. (1998). What are you looking at? Acuity for the direction of regard. *Investigative Ophthalmology and Visual Science*, *39*, S172 (Abstract 816).

Cline, M. G. (1967). The perception of where a person is looking. *American Journal of Psychology*, *80*, 41–50.

Desimone, R., & Schein, S. J. (1987). Visual properties of neurons in area V4 of the macaque: sensitivity to stimulus form. *Journal of Neurophysiology*, *57*, 835.

DeValois, R. L., & DeValois, K. K. (1988). *Spatial vision*. New York: Oxford University Press.

Dobbins, A., Zucker, S. W., & Cynader, M. S. (1987). Endstopped neurons in the visual cortex as a substrate for calculating curvature. *Nature*, *329*, 438–441.

Dobbins, A., Zucker, S. W., & Cynader, M. S. (1989). Endstopping and curvature. *Vision Research*, *29*, 1371–1387.

Gallant, J. L., Braun, J., & VanEssen, D. C. (1993). Selectivity for polar, hyperbolic, and Cartesian gratings in macaque visual cortex. *Science*, *259*, 100–103.

Gallant, J. L., Connor, C. E., Rakshit, S., Lewis, J. W., & VanEssen, D. C. (1996). Neural responses to polar, hyperbolic, and Cartesian gratings in area V4 of the macaque monkey. *Journal of Neurophysiology*, *76*, 2718–2739.

Galper, R. E., & Hochberg, J. (1971). Recognition memory for photographs of faces. *American Journal of Psychology*, *84*, 351–354.

Gibson, J. J., & Pick, A. D. (1963). Perception of another person's looking behavior. *American Journal of Psychology*, *76*, 386–394.

Glass, L. (1969). Moiré effect from random dots. *Nature*, *223*, 578–580.

Graham, N. (1989). *Visual pattern analyzers*. New York: Oxford University Press.

Hayes, T., Morrone, M. C., & Burr, D. C. (1986). Recognition of positive and negative bandpass filtered images. *Perception*, *15*, 595–602.

Kobatake, E., & Tanaka, K. (1994). Neuronal selectivities to complex object features in the ventral visual pathway of the macaque cerebral cortex. *Journal of Neurophysics*, *71*, 856–867.

Kobayashi, H., & Kohshima, S. (1997). Unique morphology of the human eye. *Nature*, *387*, 767–768.

Koenderink, J. J., & Richards, W. (1988). Two-dimensional curvature operators. *Journal of the Optical Society of America A*, *5*, 1136–1141.

Kovács, I., & Julesz, B. (1993). A closed curve is much more than an incomplete one: effect of closure in figure-ground segmentation. *Proceedings of the National Academy of Sciences*, *90*, 7495–7497.

Kovács, I., & Julesz, B. (1994). Perceptual sensitivity maps within globally defined visual shapes. *Nature*, *370*, 644–646.

Labonté, F., Shapira, Y., Cohen, P., & Faubert, J. (1996). A model for global symmetry detection in dense images. In C. W. Tyler, *Human symmetry perception and its computational analysis* (pp. 265–287). Utrecht: VSP.

Langlois, J. H., & Roggman, L. A. (1990). Attractive faces are only average. *Psychological Science*, *1*, 115–121.

Levi, D. M., Klein, S. A., & Yap, Y. L. (1988). 'Weber's law' for position: unconfounding the role of separation and eccentricity. *Vision Research*, *28*, 597–603.

Lin, L.-M., & Wilson, H. R. (1996). Fourier and non-Fourier pattern discrimination compared. *Vision Research*, submitted.

Lu, K. H. (1965). Harmonic analysis of the human face. *Biometrics*, *21*, 491–505.

Moscovich, M., & Radzins, M. (1987). Backward masking of lateralized faces by noise, pattern, and spatial frequency. *Brain and Cognition*, *6*, 72–90.

Orban, G. A., Vandenbussche, E., & Vogels, R. (1984). Human orientation discrimination tested with long stimuli. *Vision Research*, *24*, 121–128.

Phillips, R. J. (1972). Why are faces hard to recognize in photographic negative? *Perception and Psychophysics*, *12*, 425–426.

Quick, R. F. (1974). A vector-magnitude model of contrast detection. *Kybernetik*, *16*, 1299–1302.

Regan, D., & Price, P. (1986). Periodicity in orientation discrimination and the unconfounding of visual information. *Vision Research*, *26*, 1299–1302.

Schoups, A. A., Tootell, R. B., Vanduffel, W., & Orban, G. A. (1995). Use of the double-label deoxyglucose approach to map the orientation columnar system beyond area V1 and V2 in the macaque, and its plasticity. Society for Neuroscience Abstracts, 15.3.

Sinha, P., & Poggio, T. (1996). I think I know that face. *Nature*, *384*, 404.

Tanaka, J. W., & Farah, M. J. (1993). Parts and wholes in face recognition. *Quarterly Journal of Experimental Psychology*, *46A*, 225–245.

Thornhill, R., & Gangestad, S. W. (1993). Human facial beauty: averageness, symmetry, and parasite resistance. *Human Nature*, *4*, 237–269.

Tieger, T., & Ganz, L. (1979). Recognition of faces in the presence of two-dimensional sinusoidal masks. *Perception and Psychophysics*, *26*, 163–167.

Troje, N. F., & Bülthoff, H. H. (1996). Face recognition under varying poses: the role of texture and shape. *Vision Research*, *36*, 1761–1771.

Troje, N. F., & Siebeck, U. (1998). Illumination induced apparent shift in orientation of human heads. *Perception*, *27*, 671–680.

Weibull, W. A. (1951). A statistical distribution function of wide applicability. *Journal of Applied Mechanics*, *18*, 292–297.

Wilkinson, F., Wilson, H. R., & Habak, C. (1998). Detection and recognition of radial frequency patterns. *Vision Research*, *38*, 3555–3568.

Wilkinson, F., James, T. W., Wilson, H. R., Gati, J. S., Menon, R. S., & Goodale, M. A. (1999). Radial and concentric gratings selectively activate human extrastriate form areas: an fMRI study (submitted).

Wilson, H. R. (1991). Psychophysical models of spatial vision and hyperacuity. In D. Regan, *Spatial vision* (pp. 64–86). London: Macmillan.

Wilson, H. R., Ferrera, V. P., & Yo, C. (1992). Psychophysically motivated model for two-dimensional motion perception. *Visual Neuroscience*, *9*, 79–97.

Wilson, H. R., & Richards, W. A. (1992). Curvature and separation discrimination at texture boundaries. *Journal of the Optical Society of America A*, *9*, 1653–1662.

Wilson, H. R., Wilkinson, F., & Asaad, W. (1997). Concentric orientation summation in human form vision. *Vision Research*, *37*, 2325–2330.

Wilson, H. R., & Wilkinson, F. (1998). Detection of global structure in glass patterns: implications for form vision. *Vision Research*, *38*, 2933–2947.

Wilson, H. R. (1999a). *Spikes, decisions and actions: dynamical foundations of neuroscience*. Oxford: Oxford University Press.

Wilson, H. R. (1999b). Non-Fourier cortical processes in texture, form, and motion perception. In P. S. Ulinski, & E. G. Jones, *Cerebral cortex, models of cortical circuitry*, vol. 13 (pp. 445–477). New York: Plenum.

Wilson, H. R., Krupa, B., & Wilkinson, F. (1999). Dynamics of inhibition-induced oscillations in form vision (submitted).

Yin, R. K. (1969). Looking at upside down faces. *Journal of Experimental Psychology*, *81*, 141–145.

Young, A. W., Hay, D. C., McWeeny, K. H., & Ellis, A. W. (1985). Matching familiar and unfamiliar faces on internal and external features. *Perception*, *14*, 737–746.

Young, A. W., Aggleton, J. P., Hellawell, D. J., Johnson, M., Broks, P., & Hainley, J. R. (1995). Face processing impairments after amygdalotomy. *Brain*, *118*, 15–24.

Zabrodsky, H., & Algom, D. (1996). Continuous symmetry: a model for human figural perception. In C. W. Tyler, *Human symmetry perception* (pp. 289–301). Utrecht: VSP.